

CERN Summer Student Programme 2022



Thermomechanical Characteristics of Materials under  
Hypervelocity and High-Temperature Impact

– CERN Summer Student Project Report –

Monika Sharevska

CERN Summer Student,  
Faculty of Mechanical Engineering,  
Ss Cyril and Methodius University,  
Skopje, Macedonia

Supervisors

Federico Carra, PhD  
Lucie Baudin, PhD

August, 2022

Genève, Switzerland

## Contents

Abstract.....	3
1. Introduction .....	3
2. Modelling approaches .....	4
2.1. Effects of a temperature change on materials .....	4
2.2. Dynamic deformation and stress wave .....	5
3. Equation of state and constitutive models .....	7
3.1. Equation of state (EOS) .....	7
3.2. Strength models.....	9
3.3. Failure models.....	10
4. Thermomechanical phenomena in materials under beam impact .....	10
5. SESAME library for the EOS.....	12
6. Matlab code for extracting data from the SESAME library.....	14
7. AUTODYN simulations.....	23
8. Conclusions .....	25
References .....	26

# Thermomechanical Characteristics of Materials under Hypervelocity and High-Temperature Impact

Monika Sharevska, CERN Summer Student

## Abstract

The thermomechanical characteristics of materials under hypervelocity and high-temperature impact are analyzed. Thermodynamic states of high compression and expansion are produced. Thermomechanical phenomena connected with high pressures and temperatures, elastic, plastic and shock wave behavior, changes of material density, phase (solid-liquid-gas-plasma) transitions, intense stress waves, material fragmentation and explosions, are discussed. Matlab code is created in this work, and equation of state diagrams are presented using SESAME equation of state files. Simulation of laser beam impact on various materials using different EOS is conducted and results are discussed.

**Key words:** Equation of state, SESAME library, hadron beam impact, material response, MATLAB code, simulation

## 1. Introduction

The subject of this work is thermomechanical characteristics of materials under hypervelocity and high-temperature impact. The mechanical energy of the hypervelocity projectiles is dissipated and converted in thermal energy causing high temperatures on the target. The definition of the material equation of state (EOS) is essentially important for analysis and solution of the thermomechanical problems.

The thermomechanical and physical processes important to hypervelocity impact phenomena are discussed by Asay and Kerley (Sandia National Laboratories) [1], where a perspective of theoretical foundation is presented and an overview of equation of state and constitutive modeling capabilities are provided. A study of the thermomechanical response of materials to a time-dependent heat load is given by Carra [2] and Carra *et al.* (CERN) [3,4]. Theoretical, numerical, and experimental investigations are conducted. The investigations are focused on quasi-instantaneous heating. Numerical codes are developed, analytical methods and experimental tests in particle accelerator facilities are performed. A simulation model for material response under laser beam impact and a comparison of different equations of state are given by Baudin (CERN) [5,6]. The investigations presented by Martin *et al.* [7] show the spalling in tantalum, which has been observed in an experiment at CERN's HiRadMat Facility. The SESAME EOS Library [8] is a standardized, computer-based library of tables for the thermodynamic properties of materials, developed and maintained by the Mechanics of Materials and Equation-of-State Group (T-1) of the Theoretical Division at Los Alamos National Laboratory.

In order to extract data from the SESAME file and to create properties diagrams for the materials, a Matlab code is created in this work, and equation of state diagrams for various materials are presented.

The equation of state of gases (ideal and real), vapors and liquids, and evaporation, condensation, sublimation and de-sublimation processes [9] were part of my education at the Faculty of Mechanical Engineering, Department of Thermal and Power Engineering.

As a student at CERN Summer Student Programme I am introduced to EOS of materials, thermomechanical response of materials under hypervelocity and high temperature impact, and theoretical, computational, and experimental methods of investigations, which is the main purpose of my study at CERN.

The purpose of this work is to present the basic knowledge of EOS of materials, and thermomechanical response of materials under hypervelocity and high temperature impact. The particular purpose is to create Matlab code, to present equation of state diagrams for various materials, to make some simple numerical experiments and to analyze results.

## 2. Modelling approaches

### 2.1. Effects of a temperature change on materials

A change of temperature in a component, induces deformations, strains and stresses which can potentially lead to the component failure. The thermomechanical problems can be group into [2]:

- Quasi-static heating: the variation of temperature over time is negligible and the temperature gradient for a given load depends on the material thermal conductivity.
- Slow-transient heating: the variation of temperature over time is non-negligible, but the heating rate is low enough to allow dynamic effects due to mass inertia of the structure to be neglected.
- Quasi-instantaneous heating: when the heating occurs in a very short time, the core material expansion is prevented by its mass inertia. The thermal energy deposition on a body induces temperature and pressure increase. Pressure waves are generated.

The energy density induced on the material by proton, ion and electron beams impact is similar to the brightest lasers. The laser penetration depth depends on the wavelength and on the absorption coefficient of the target ( $10^{-9}$ – $10^{-6}$  m). Hadron beams of particle accelerators penetrate much deeper inside the impacted material. In the LHC the circulating proton beam would penetrate 10–15 m in the case of a head-on impact on a carbon structure. The beam is swept along a spiral pattern using pulsed magnets. 8 m – long graphite cylindrical component is the dump. Figure 1 presents temperature distribution on the LHC dump [4].

The material dynamic response depends on the total amount of energy deposited, its distribution, the duration of the impact, the thermophysical and mechanical properties of the material, and the form and dimensions of the device interacting with the beam.

Plot of maximum deposited power versus duration of deposition, showing the different dynamic responses that can be induced in matter by interaction with particle beams is given in Figure 2 [10]. Points represent cases of beam impacts (real or simulated).

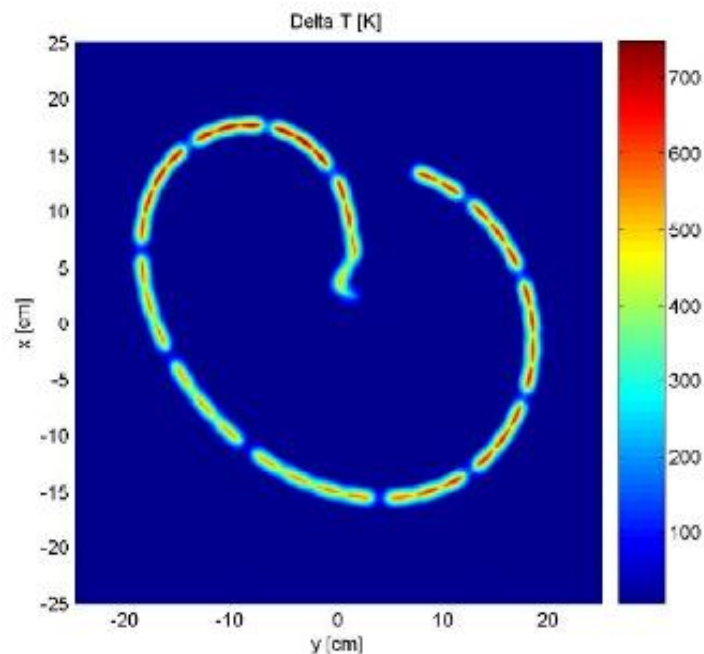


Figure 1 Temperature distribution on the LHC dump [4]

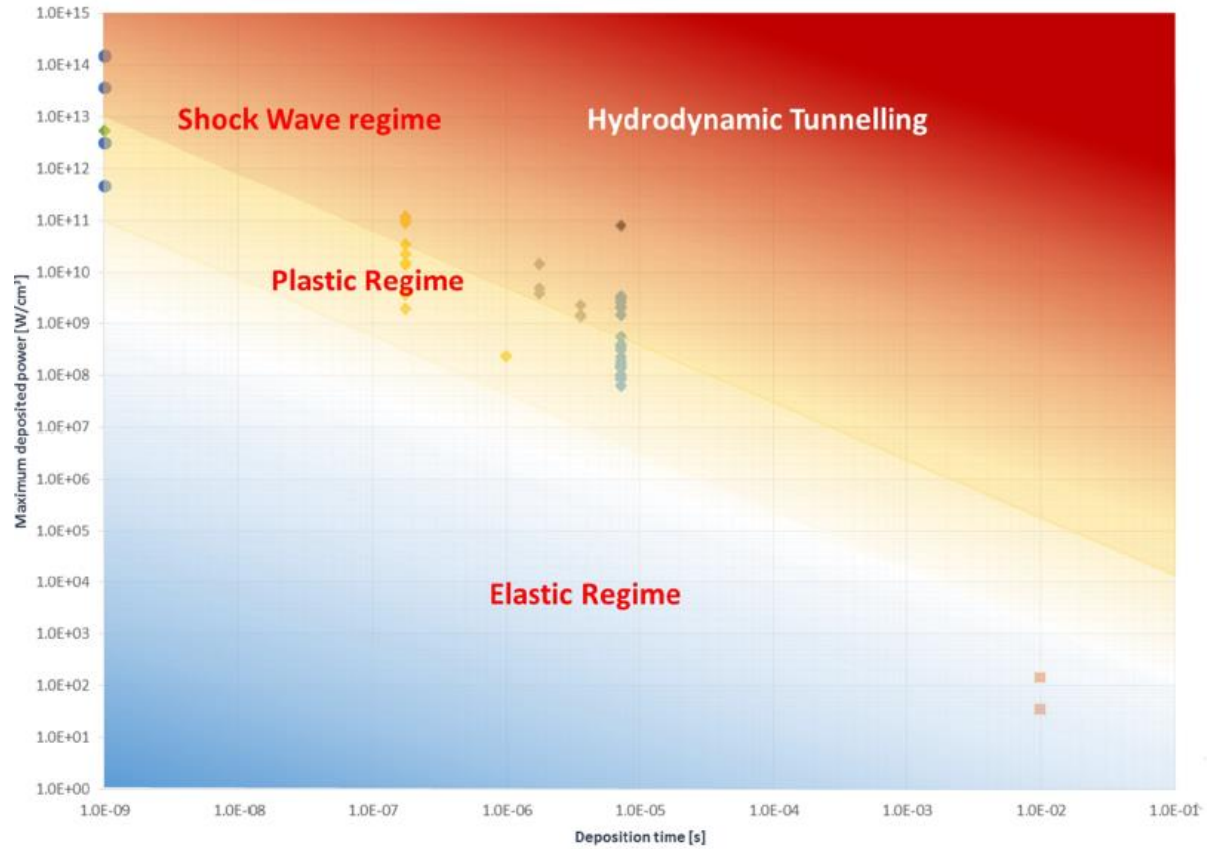


Figure 2 Plot of maximum deposited power versus duration of deposition, showing the different dynamic responses that can be induced in matter by interaction with particle beams. Points represent cases of beam impacts (real or simulated) [10].

## 2.2. Dynamic deformation and stress wave

**Elastic waves.** The relation between stress and strain in the elastic domain is expressed by Hooke's law. Velocity of an elastic wave is equal to speed of sound  $c_0$ .

**Plastic waves.** The stress amplitude is over the elastic limit of the material and the wave decomposes into an elastic and a plastic wave. The plastic wave propagates at a speed lower than  $c_0$ .

**Shock waves.** The function slope  $\partial\sigma / \partial\epsilon$  increases with the plastic strain (Figure 6). For very high amplitudes of the pressure wave, a discontinuity in pressure is generated - shock front. The shock wave speed is higher than the initial speed of sound.

**Hydrodynamic material state.** The solid is assumed to behave like a fluid, no phase transformations, body forces and heat conduction is assumed. Figure 3 illustrates the material state ahead and behind the shock front. The center of the reference system is the shock front. The material ahead is in an unshocked condition of  $p_0$ ,  $T_0$  and  $\rho_0$ , with null velocity  $U_0$ . The shocked material is at  $p$ ,  $T$  and  $\rho$ , and moves with velocity  $U_p$ . The relative velocity of the front with respect to the unshocked material is  $U_s - U_0 = U_s$ . Combining the conservation laws for mass, momentum and energy the energy generated by the shock as a function of the other quantities is,

$$E - E_0 = \frac{1}{2}(p + p_0) \left( \frac{1}{\rho_0} - \frac{1}{\rho} \right) \quad 1$$

This form of the energy conservation is known as Hugoniot equation.

The system is of three equations (mass, momentum, and energy conservation). An additional equation between  $U_s$  and  $U_p$  is needed in order to determine all the parameters as a function of one of them. This fourth equation has different forms, the most common ones relating  $U_s$  and  $U_p$ , or  $E$ ,  $p$  and  $\rho$ , and is defined as the equation of state (EOS) of the material,

$$U_s = C_0 + S_1 U_p + S_2 U_p^2 + \dots + S_n U_p^n \quad p = f(\rho, E) \quad 2$$

with  $C_0$  equal to the sound speed of the unstressed material and  $S_1, S_2, \dots, S_n$  parameters of the polynomial expression. When phase changes do not occur, a linear equation of state describes sufficiently well the shock response of the material.

$$U_s = C_0 + S_1 U_p \quad p = K \left( \frac{\rho}{\rho_0} - 1 \right) + \gamma_0 E \quad 3$$

where  $\gamma_0$  is the Grüneisen parameter.

The Hugoniot equation (1) is shown graphically in the  $p$ - $v$  diagram of Figure 4. The loading during the shock occurs along the Rayleigh line. The unloading follows the isentrope path, which is close to the Hugoniot curve. The applied load is of finite duration. A rarefaction wave is generated after the load removal. Any signal travelling in the shocked volume is faster than the compressive wave, the rarefaction wave reaches and attenuate the amplitude of the compression.

**Shock in elastoplastic materials.** The elastoplastic behavior of the material (shear and strength) cannot be neglected. The Hugoniot curve shown in Figure 4 must be updated to keep into account the deviatoric component of the stress. The physical condition under which shock waves can develop is uniaxial strain. In this case, the  $\sigma - \epsilon$  curve becomes convex (Figure 5). The yield stress in uniaxial strain condition is usually indicated with  $\sigma_{HEL}$ , or Hugoniot elastic limit.

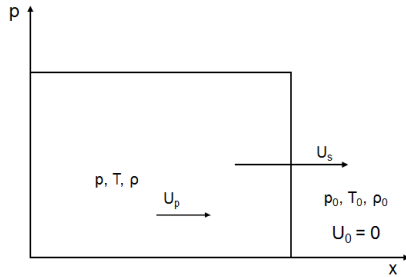


Figure 3 Shock front, hydrodynamic treatment

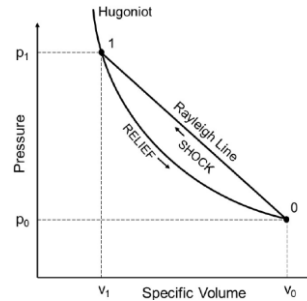


Figure 4 Characteristic Hugoniot curve and Rayleigh line in the pressure - specific volume diagram

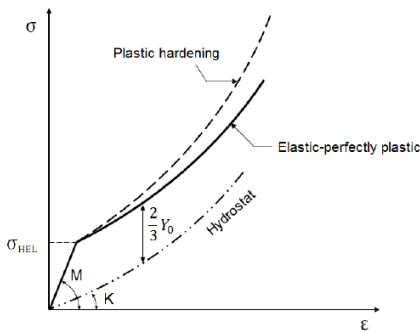


Figure 5  $\sigma - \epsilon$  curve for a material in uniaxial strain conditions

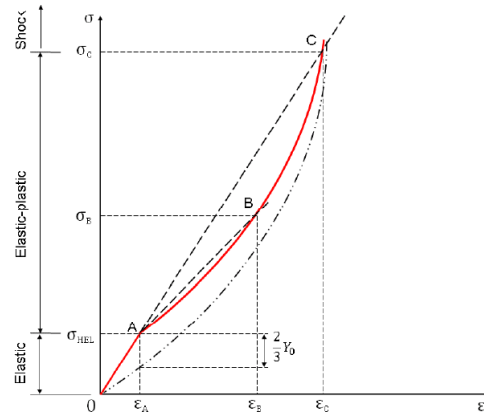


Figure 6 Hugoniot curve in stress and strain coordinates for an elastic-perfectly plastic material

In uniaxial strain conditions, the velocity of plastic waves is initially lower than that of elastic waves, but it increases with the stress creating the conditions for the generation of a shock front. This concept can be explained graphically by the Hugoniot curve, in stress and strain coordinates (Figure 6).

**Thermally-induced shock waves.** The critical stress causing the generation of shock waves can be reached with mechanical impact or with isochoric heating (Figure 10). The shape of the energy deposition on the matter follows the proton beam trajectory, with a peak along the beam axis, and a Gaussian distribution in the material transversal sections. The waves generated by the impact present a cylindrical pattern and the amplitude of cylindrical waves rapidly decreases during the expansion inside the impacted material.

**Hydrodynamic tunneling.** In the solid state a rarefaction wave grows at the impacted volume and follows the compressive wave. The result is density decrease, such that subsequent bunches impact on a less dense material, penetrating deeper in the matter.

### 3. Equation of state and constitutive models

The term equation of state (EOS) is used when: referring to equilibrium hydrostatic behavior, while everything else is constitutive response or model (Figure 7) [1]. The EOS models are developed using: numerical continuum mechanics (conservation of mass, momentum and energy); statistical mechanics theory and experimental data; fundamental methods in regimes inaccessible to experiment. Constitutive modeling starts by assuming a known EOS. Phenomenological correction using experimental data is used. Experimental work has led to improve understanding of the microscopic aspects of material response.

#### 3.1. Equation of state (EOS)

The typical form of an EOS is a relation between pressure, density and energy, or between the shock velocity and the particle velocity (Eq. 2). An EOS can be expressed relating any two independent variables among  $p$ ,  $v$  (or  $\rho$ ),  $E$  (or  $T$ ),  $U_s$ ,  $U_p$ . The knowledge of the specific heat capacity  $c_v$  is required to express the temperature as a function of the energy.

The most well-known and simplest EOS is the ideal gas law, expressing the relation between pressure, volume and temperature. In real materials, equations of state are much more complex. In particular, the changes of phase have to be considered, and the Hugoniot curve becomes of the form qualitatively sketched in the  $T, \rho$  plane, for a fictitious material (Figure 8). The following regions should be determined in constructing an equation of state: solid phase; liquid phase; coexistence region solid/liquid/gas; gas phase; plasma phase; transition regions.

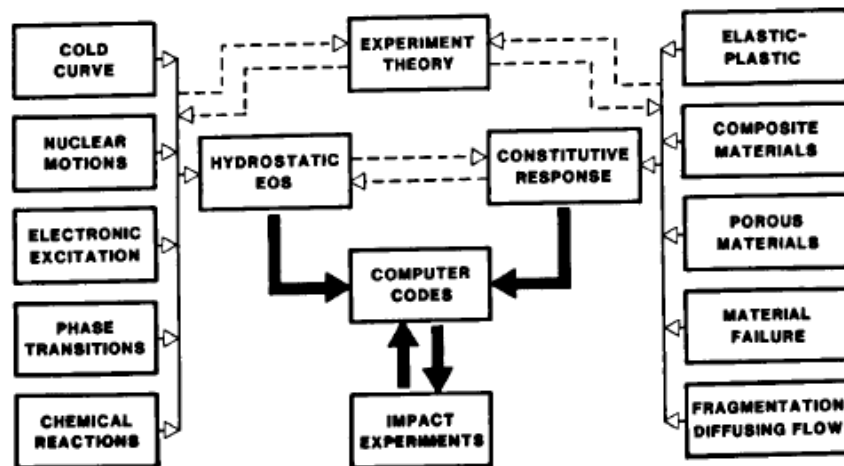


Figure 7 Steps in constructing a model of dynamic material response [1]

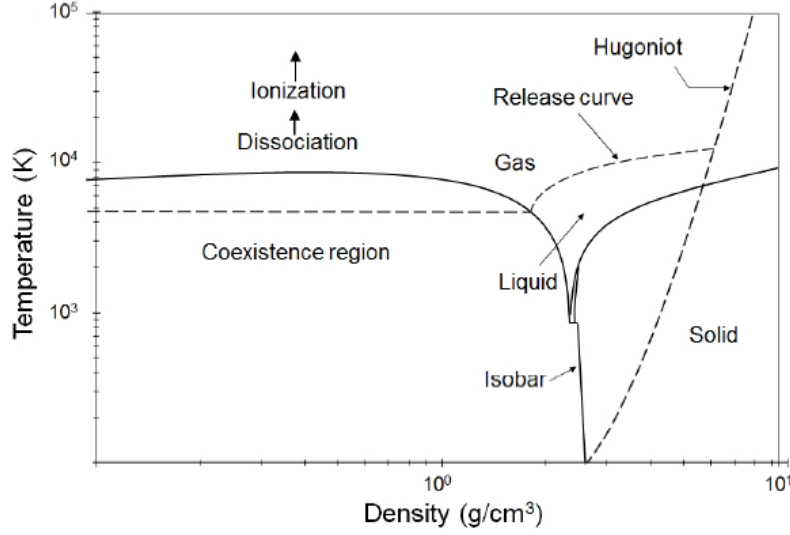


Figure 8 Regions of interest in an EOS of a fictitious material

**EOS reference to the cold curve.** The cold curve is defined as the region of the pressure, density, temperature diagram corresponding with the 0 K isotherm. Numerical codes (Ansys AUTODYN) usually express the equation of state as a sum of two components:

$$p = p_c(\rho) + p_T(\rho, E) \quad 4$$

where  $p_c$  represents the cold curve, while the second term  $p_T$  is energy (temperature) dependent.

If the material regime that can be reached experimentally by isochoric heating with no change of phase is typically below the shock threshold, a linear pressure – density EOS describes fairly well the material response when no phase transformations are involved. An extension of linear EOS is the Mie-Grüneisen, which can be applied to a certain extent also in the liquid phase [4]. This EOS is the base for the derivation of EOS for alloys, mixtures and porous materials. When the energies involved in the shock lead to the generation of gas or plasma, or when several solid phases exist in addition to the liquid, separate EOS are built for each phase, locating the phase boundaries by matching free energies. EOS computed in this way are usually expressed in tabular form. An example is the SESAME EOS [8], developed and maintained by the Los Alamos National Laboratory (US).

**Linear EOS.** This simple equation of state expresses the relation between pressure and density with a linear function. With reference to Eq. (4), the cold curve has the following form,

$$p_c(\rho) = K \left( \frac{\rho}{\rho_0} - 1 \right) \quad 5$$

The proportionality constant is therefore represented by the Bulk modulus. The energy-dependent component of the EOS is:

$$p_T(\rho, E) = \gamma_0 E \quad 6$$

where  $\gamma_0$  is the Grüneisen parameter calculated at  $\rho_0$ :

$$\gamma_0 = \frac{\alpha K}{\rho_0 c_v}$$

Combining Eq. (5) and (6), the general expression of the linear EOS is derived:

$$p(\rho, E) = K \left( \frac{\rho}{\rho_0} - 1 \right) + \gamma_0 E \quad 7$$



**Mie-Grüneisen EOS.** The Mie-Grüneisen approximation is a powerful tool for describing an equation of state, because of its simplicity and the fact that it can be directly fit to experimental data without using theoretical models. It is expressed by the relation:

$$p = \frac{\rho_0 C_0^2 \left( \frac{\mu}{\mu + 1} \right)}{\left( 1 - S \left( \frac{\mu}{\mu + 1} \right) \right)^2}; \mu = \frac{\rho}{\rho_0} - 1 \quad 8$$

where  $\rho_0$  – normal density (g/cm<sup>3</sup>),  $C_0$  – speed of sound (km/s),  $S$  – material constant, slope of  $U_s$ - $U_p$  curve. Mie-Grüneisen EOS is adopted and applied for porous materials and for compounds and alloys [5].

**Tabular EOS.** The most sophisticated form of equation of state is the tabular EOS. A tabular form allows expressing strong nonlinearities and discontinuities, and is typically the best choice when the material is expected to experience important variations in density and energy, as well as changes of phase. A generic tabular equation is shown in Figure 9.

**Conventional experimental methods.** The experiments are used to test theoretical assumptions for EOS and to determine where the EOS need to be improved. Application of the more fundamental methods should increase confidence in the EOS in regimes inaccessible to experiment.

**EOS study by isochoric heating test.** A novel method for the study of the EOS regions which are usually inaccessible to conventional experiments is proposed [2], based on a quasi-instantaneous heating of the material produced by the impact of an intense proton beam. This concept is graphically seen in Figure 10.

### 3.2. Strength models

The real materials exhibit a shear strength, as well as hardening or softening as functions of strain, strain rate and temperature, the deviatoric component of the stress cannot be ignored. This is very important in the case of a plastic wave below the critical shock stress, and where the hydrostatic component of the stress becomes of the same order of magnitude of the shear and strength.

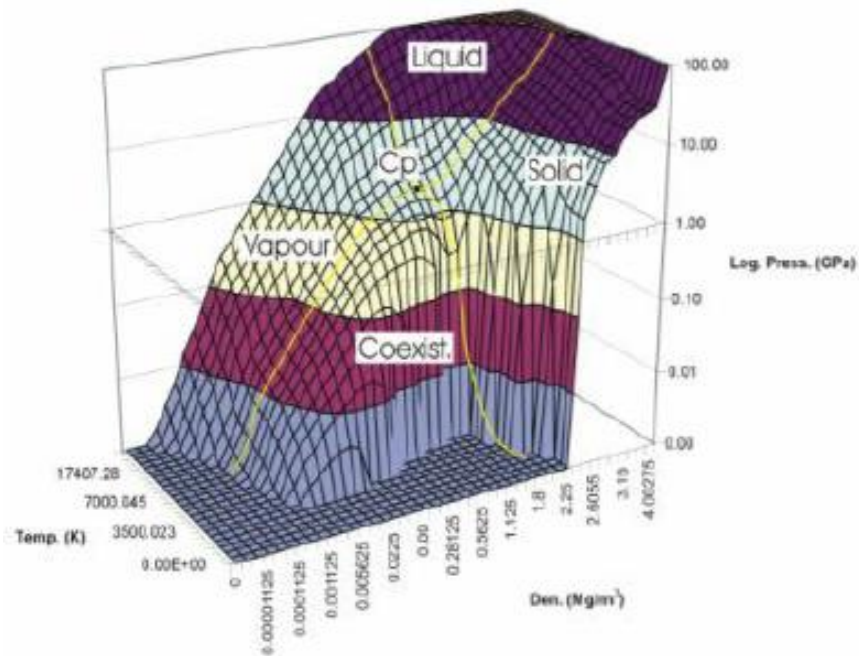


Figure 9 Example of tabular equation of state. The different phases are highlighted

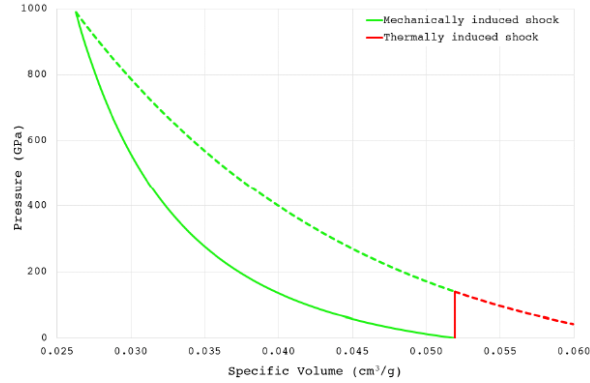


Figure 10 Shock on a tungsten target. In green, the shock is induced by a mechanical impact, in red, by a thermal energy deposition. Continuous lines are referred to the load phase and dashed lines to the release phase [2]

### 3.3. Failure models

The two main failure models are:

- failure as a result of cumulative damage,
- material fracture by spallation

Spallation is a dynamic phenomenon [7]. The amplitude of a rarefaction wave exceeds the ultimate strength of the material and internal cavitation occurs. Fragments, or spalls, are formed, and ejected far from the surface at high speed.

## 4. Thermomechanical phenomena in materials under beam impact

The impact of the proton or ion beams causes complex thermomechanical phenomena in a target. If the beam pulse is sufficiently intense, extreme conditions can be reached: very high pressures and temperatures, changes of material density, phase transitions, stress waves, material fragmentation and explosions. The beam dump absorbs the energy of particles within an energetic beam. The kinetic energy of the beam, which travels at relativistic speed, is partially or totally transferred to the target material in the form of heat. The heating occurs in a very short time - quasi-instantaneous heating.

The energy density peak decreases in amplitude and increases in depth with the decrease of the material density and atomic number. Hadron beams penetrate inside the impacted material. The penetration depth is mostly depended on: the beam transverse section and intensity; the particle nature and energy; and the density and atomic number of the target (Figure 11 and Figure 12).

New composites were developed at CERN in recent years to replace the carbon-fibre-reinforced carbon (CFC) currently adopted in the present LHC, combining the good thermal and electrical properties of metals with the high thermal stability of carbon allotropes such as graphite and diamond. The most promising are Copper-Diamond (CuCD) and Molybdenum-Graphite (MoGr) [3,4].

The modelling of the change of phase is related to the EOS of the material. In the case of vaporization, a single EOS describes both the vapor and the condensed phase. 3D  $p$ - $v$ - $T$  surface for copper is given in Figure 13 [4]. In the figure the labels mean: M, melting region; R, evaporating region with the critical point, CP; solid, liquid, gas, liquid + gas, and plasma (arrows indicate the decrease in plasma nonideality parameter) physical states; H1 and Hp, principal and porous Hugoniot; S, release isentropes of shock-compressed metal; IEX, isobaric expansion; DAC, static compression in diamond anvil cells; LM, density of liquid metal at room pressure; and LHC, states generated in copper by the LHC beam covering strongly coupled plasma region.

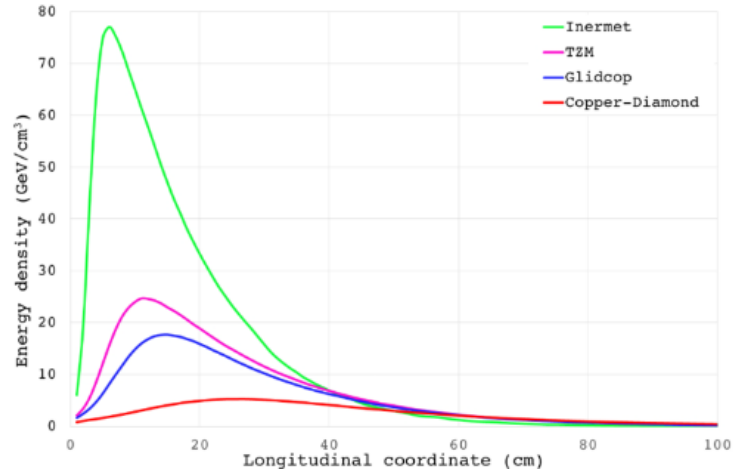


Figure 11 Energy density generated by a proton beam impact on a cylindrical target made of different materials



Figure 12 Results from HiRadMat's 2012 experiment on different material specimens' response under high-energy, high-intensity beams (From left to right: Inermet 180, molybdenum, Glidcop, molybdenum-copper-diamond, copper-diamond, molybdenum-graphite (three different grades))

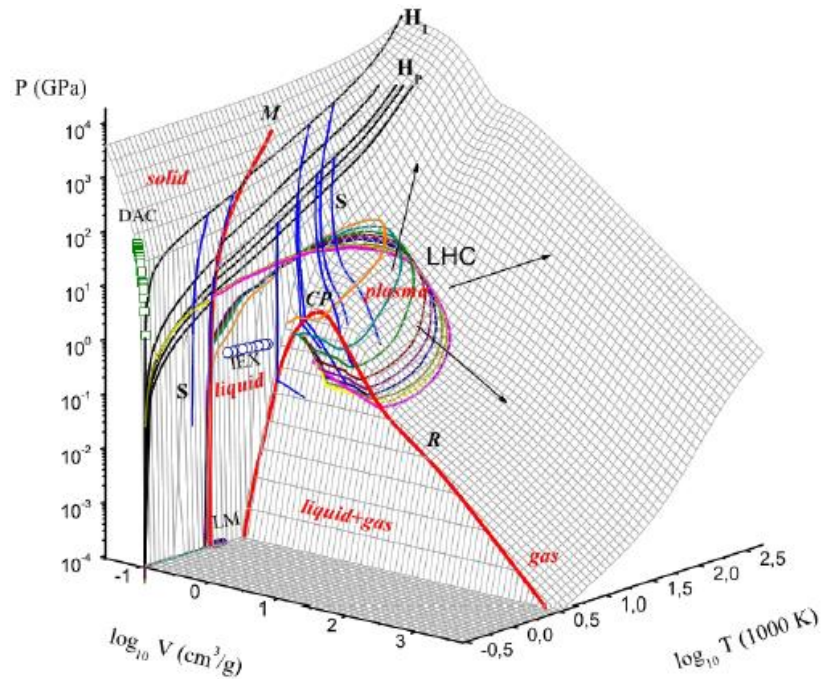


Figure 13 3D p-v-T surface for copper

## 5. SESAME library for the EOS

The most sophisticated form of equation of state is the tabular EOS. A tabular form allows expressing strong nonlinearities and discontinuities, and is the best choice when the material is expected to experience important variations in density and energy, as well as changes of phase. The SESAME Equation-of-State (EOS) Library is a standardized, computer-based library of tables for the thermodynamic properties of materials. The SESAME EOS Library is developed and maintained by the Mechanics of Materials and Equation-of-State Group of the Theoretical Division at Los Alamos National Laboratory. The library currently contains data for about 250 materials, including simple elements, compounds, metals, minerals, polymers, mixtures, etc. The EOS's for existing materials in the library are upgraded, and EOS's for new materials are added frequently. Expansive regions of pressure and temperature are implemented. Some particular applications include stellar and planetary modelling, as well as implementation in hydrodynamics simulations. Equations of state are formed using various combinations of different theoretical models in different regions with interpolation between. The use of the SESAME EOS is advantageous in numerical codes. The SESAME library is directly integrated in Ansys AUTODYN.

The SESAME library consists of tables for different materials organized in a dat/ascii file. The Old SESAME Library is organized in a dat file and consists of 15-digit numbers, whereas the New SESAME Library is organized in an ascii file and consists of 22-digit numbers. The procedure of reading the SESAME table is shown on Figure 14. The first line indicates the material number and the table number. In the SESAME Manual there is a list of all the materials and their corresponding material number. For example, calcium number is 2030. Tables 101, 102 and 103 are comments. Table 201 shows the mean atomic number, mean atomic mass, normal (solid) density, solid bulk modulus and exchange coefficient. The equation of state is presented in table 301, which is composed by the zero-temperature isotherm (cold curve), the thermal ionic, and thermal electronic.

A comparison between the Old SESAME Library and the New SESAME Library was made. The New SESAME Library has all the previous material tables shown in the Old SESAME Library and several new materials are added. The list of the new materials with the date of last update is shown in Table 1. The latest update is in April 2017. Particularly valuable is the new table for copper – 3337, because of its application as material for the beam dump. EOS of alloys are added, for example Nickel-Copper alloy. Most of the materials used as a beam dump are mixtures. Building an EOS for mixtures requires knowledge of the EOS of the constituents, as well as the weight ratio.

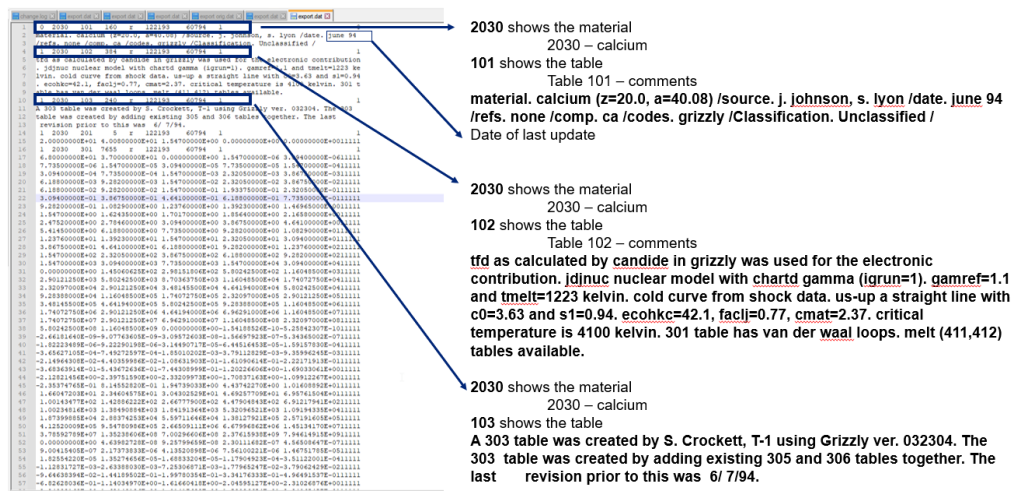


Figure 14a





Table 1 New materials in the New SESAME Library

Name	Materials in New sesame	Date of the last update
Scandium	2100	Jul-12
silver	2721	May-11
Ti-Beta-21S	2963	Dec-09
copper	3337	Oct-11
Platinum	3731	Apr-17
Nickel-Copper alloy	4210	Jul-07
argon	5173	Aug-12
xenon	5191	Mar-10
carbon dioxide	5212	Sep-07
Deuterium	5266	Feb-04
Deuterium	5267	Sep-07
Titanium Hydride	6013	Apr-09
Cesium Iodide	6020	Sep-10
Polyethylene	7173	Apr-17
Poly(ethylene-vinyl acetate-vinyl alcohol) (VCE) reactant (inert)	7940	Dec-06
Poly(ethylene-vinyl acetate-vinyl alcohol) (VCE) Products	7941	Dec-06
s5370-reactant (inert)	7970	Mar-07
s5370 products	7971	Jun-07
sx358-reactant (inert)	7980	Mar-07
sx358-products	7981	Jun-07

## 6. Matlab code for extracting data from the SESAME library

In order to extract data from the SESAME Library and create properties diagrams for the materials, a Matlab code is created. The code provides the temperature and density arrays and the corresponding pressure and internal energy of each combination of temperature and density. A point is defined by its temperature and density. The other properties depend on the temperature and density. Matrices for the pressure and internal energy are created. The number of cells in the matrix (the multiplication of number of densities and number of temperatures) is the number of points in the SESAME library (Table 2).

The Matlab code enables a selection of preferred range of temperature and density and extraction of the points in ranges (Table 2). When a beam impact on a target occurs, extremely high temperatures are obtained. The range of interest is defined between room temperature and 4000 K. The range of interest of density is defined between half of the normal density of the material and twice the normal density of the material. The number of points in the ranges of interest are calculated.

In the SESAME library expansive regions of pressure and temperature are implemented. The SESAME library can be used for simulation of a hypervelocity high-temperature impact on a target in Ansys AUTODYN. Calculation of the number of points in the range of interest is important for determination of the accuracy of the EOS in that region. Higher number of points in the range of interest leads to more accurate EOS. If the number of points in the range of interest is insufficient, the SESAME EOS should not be used for the simulation and different EOS should be chosen.

Using the Matlab code, the points in the range of interest are extracted and diagrams are created.

The Matlab code input is the material name, material number, the start row, the end row and the ranges of interest for density and temperature. The start and end row define the rows in which the table for the chosen material starts and ends. These define the lines that are read by the Matlab code. They need to be entered manually after looking at the dat/ascii file.

The Matlab code output is the minimum and maximum density, the number of densities, the minimum and maximum temperatures, the number of temperatures and the number of points in the table, as well as the number of temperatures, densities and points in the range of interest (Table 2).

Table 2 Matlab code results

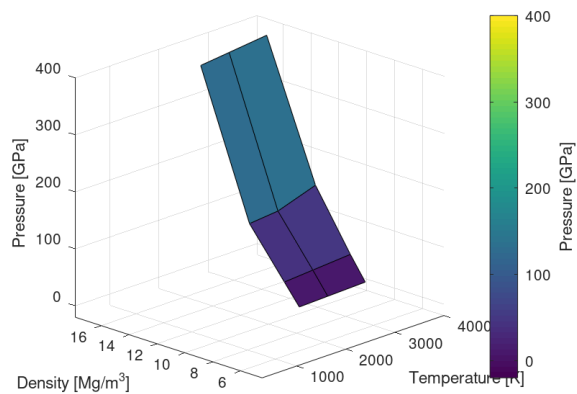
Material	Material number	startRow	endRow	Density [g/cm <sup>3</sup> ]		Number of densities	Temperature [K]		Number of temperatures	Number of points	Normal Density	Range of Temperature of Interest [K]		Range of Densities of Interest [g/cm <sup>3</sup> ]		Number of temperatures	Number of densities in the	Number of points in the
				Min	Max		Min	Max				from	to	from	to			
Diamond	7830	1242942	1243896	0.35238	352.38	93	0	371360000	25	2325	3.50998	293.15	4000	1.75499	7.01996	1	20	20
'Carbon (Tahir)'	0	0	0	0	0	0	0	0	0	0	2.28	293.15	4000	1.14	4.56	0	0	0
'Carbon liquid'	7831	1246831	1247716	0.23	100	48	0	10000000	30	1440	3.68775269	293.15	4000	1.843876345	7.37550538	9	25	225
'Carbon graphite'	7832	1247736	1249746	0	45000	72	0	1160500000	46	3312	2.25	293.15	4000	1.125	4.5	5	17	85
'Carbon graphite'	7833	1255266	1257276	0	45000	72	0	1160500000	46	3312	2.25	293.15	4000	1.125	4.5	5	17	85
'tungsten'	3541	0	0	0	0	0	0	0	0	0	19.25	293.15	4000	9.625	38.5	0	0	0
'molybdenum'	2980	290268	291221	0	204000	101	0	371360000	23	2323	10.2	293.15	4000	5.1	20.4	3	29	87
'molybdenum'	2981	294165	294656	8.5	1000	47	50	1160500	17	799	10.2	293.15	4000	5.1	20.4	5	26	130
'molybdenum'	2983	294707	294908	10.2	250	15	0	2310900	32	480	10.2	293.15	4000	5.1	20.4	3	4	12
'molybdenum'	2984	295545	297070	0	51100	66	0	1160500000	38	2508	10.2	293.15	4000	5.1	20.4	4	13	52
'carbonium'	3520	0	0	0	0	0	0	0	0	0	0	0	0	0	0	0	0	0
'beryllium'	2020	0	0	0	0	0	0	0	0	0	0	0	0	0	0	0	0	0
'water'	7150	903021	904453	0.000002	400	80	290.12	174070000	44	3520	0.9982	293.15	4000	0.4991	1.9964	12	13	156
'water'	7152	904462	905859	0.00000001	1.4	74	250	4000	31	2294	0.9982	293.15	4000	0.4991	1.9964	27	23	621
'water'	7153	905891	907421	0	19964	68	0	1160500000	37	2516	0.9982	293.15	4000	0.4991	1.9964	4	13	52
'water'	7154	907444	908929	0	4990	66	0	1160500000	37	2442	0.9982	293.15	4000	0.4991	1.9964	4	13	52
'Silica not found'	0	0	0	0	0	0	0	0	0	0	0	0	0	0	0	0	0	0
'Stainless steel'	4270	591848	592792	0.061687	157920	100	0	371360000	23	2300	7.896	293.15	4000	3.948	15.792	3	29	87
'Stainless steel'	4271	595705	597435	0	39550	73	0	1160500000	39	2847	7.896	293.15	4000	3.948	15.792	6	19	114
'titanium alloy'	2951	245366	246985	0	88940	72	0	1160500000	37	2654	4.447	293.15	4000	2.2235	8.894	4	17	68
'titanium alloy'	2962	251591	253188	0	88380	71	0	1160500000	37	2627	4.447	293.15	4000	2.2235	8.894	4	16	64
'Niobium'	2740	219976	221506	0	171600	68	0	1160500000	37	2516	8.58	293.15	4000	4.29	17.16	4	13	52
'Copper'	3332	358621	358886	8.93	1000	22	0	11604000	29	638	8.93	293.15	4000	4.465	17.86	3	4	12
'Copper'	3333	359720	361672	0	1000	74	0	58020000	65	4810	8.93	293.15	4000	4.465	17.86	12	13	156
'Copper'	3334	361693	363983	0.02	10	90	293	11000	60	5400	8.93	293.15	4000	4.465	17.86	32	42	1344
'Copper'	3337	378389	384944	0	178750	118	0	1160500000	92	10856	8.93	293.15	4000	4.465	17.86	31	32	992
'Aluminum'	3713	423941	424147	2.7	100	17	0	11604000	29	493	2.7	293.15	4000	1.35	5.4	3	4	12
'Aluminum'	3715	424805	426955	0	1000	100	0	116040000	53	5300	2.7	293.15	4000	1.35	5.4	12	21	252
'Aluminum'	3716	426979	427791	0.001	1000	86	300	18567	23	1978	2.7	293.15	4000	1.35	5.4	16	23	368
'Aluminum'	3717	427807	430324	0	54000	83	0	1160500000	50	4150	2.7	293.15	4000	1.35	5.4	13	21	273
'Aluminum'	3718	436866	439823	0	27	66	0	1160500000	74	4884	2.7	293.15	4000	1.35	5.4	26	21	546
'Aluminum'	3719	447252	450210	0	27	66	0	1160500000	74	4884	2.7	293.15	4000	1.35	5.4	26	21	546
'TiN not found'	0	0	0	0	0	0	0	0	0	0	0	0	0	0	0	0	0	0
Dry air	5030	627160	627432	0.00000001	15	21	175.24	348150000	31	651	0.001293	293.15	4000	0.0006465	0.002586	4	1	4

There are three tables 301 for copper in the Old SESAME table (tables 3332, 3333 and 3334) and four in the New SESAME table. A new table for copper – 3337 is added in the New SESAME library. A comparison between the different tables for copper was made.

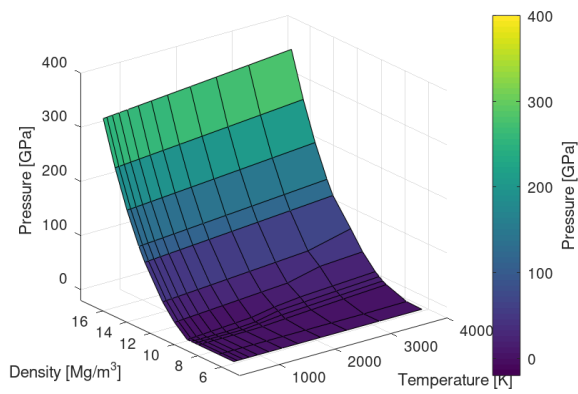
Temperature – Density – Pressure diagrams in the range of interest are shown on Figure 15. Table copper 3332 cannot be used for accurate equation of state, because of the low number of points in the range of interest - 12 points (Table 2). The number of points in the range of interest in table copper 3334 is the highest – 1344 points. However, the maximum density in table copper 3334 is 10 g/cm<sup>3</sup>. The upper limit of the range of interest is 17.86 g/cm<sup>3</sup>. The area from 10 to 17.86 g/cm<sup>3</sup> is not covered by Table 3334. The new table for copper – table 3337 covers the whole range of interest and has relatively large number of points – 992 points.

For simulation in AUTODYN the new table for copper – 3337 should be used. Table 3337 has not been integrated in AUTODYN yet. The procedure of adding new tables in AUTODYN is complex. Instead of adding the new table in AUTODYN, table 3334 could be used for density up to 10 g/cm<sup>3</sup> and table 3333 for higher densities.

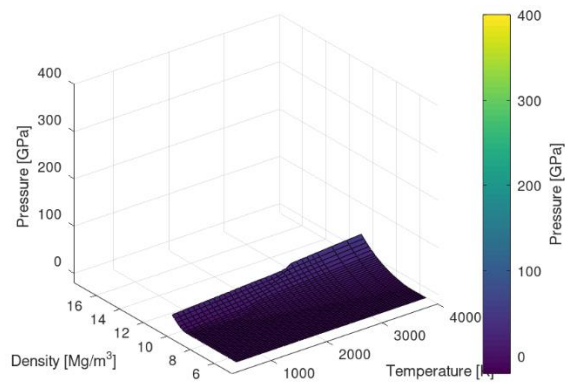
Density – Pressure diagrams in the range of interest for different tables for copper were created (Figure 16). Table copper 3333 has higher number of temperatures in the range of interest than table copper 3332. The number was reduced to 7 isotherms for better visualization. The influence of the temperature on the EOS is relatively low. The zoomed diagrams are shown on Figure 17. In the area below the normal density (8.93 g/cm<sup>3</sup> for copper) and around 0 GPa pressure, the isotherms are vertical in tables 3333 and 3334. Table copper 3337 has more data in the area of low pressure and low density. Negative pressure is the result of a tensile force on the material. The data from table copper 3337 match with Mie-Gruneisen EOS in the area of low pressure and low density (see end of this section). For simulation of a tensile force on the material table 3337 should be added in AUTODYN, or Mie-Gruneisen EOS could be used.



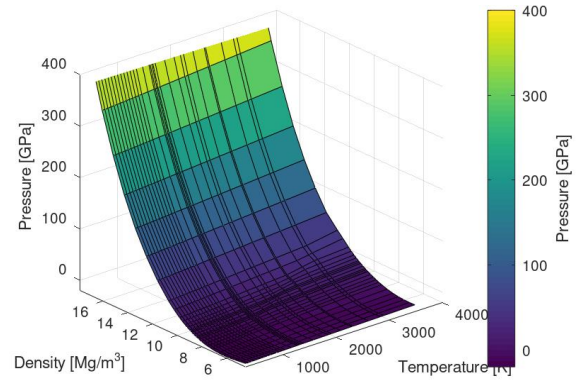
A) Copper 3332



B) Copper 3333



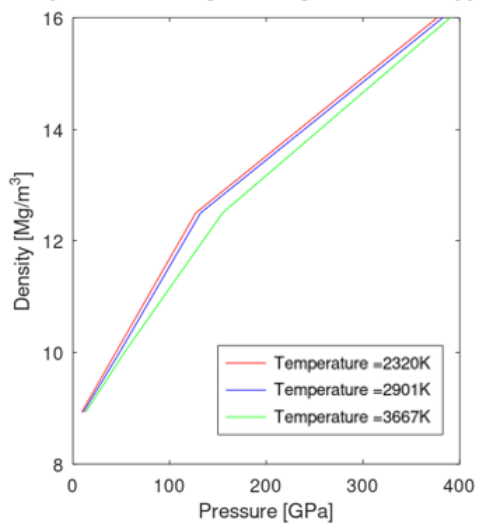
C) Copper 3334



D) Copper 3337

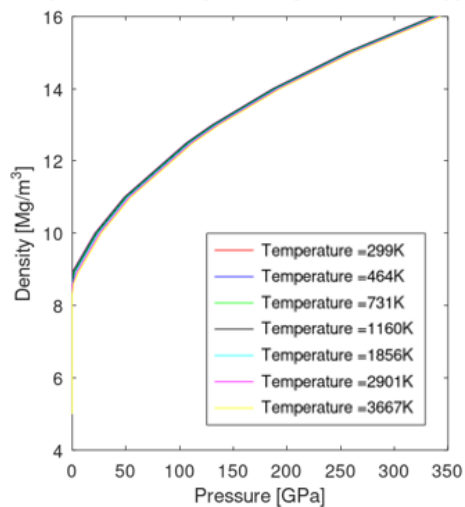
Figure 15 Temperature – Density – Pressure diagrams in the range of interest for different copper tables

Density - Pressure Diagram Range of interestCopper3332



A) Copper 3332

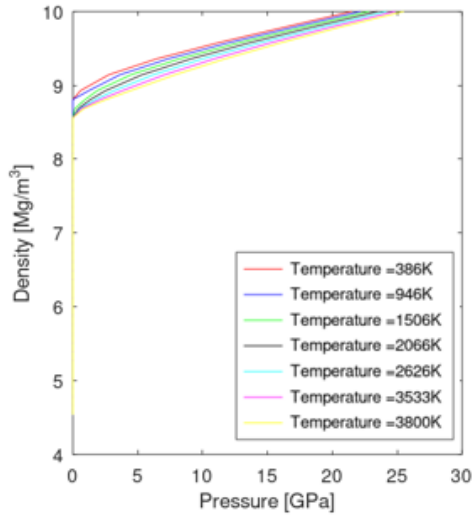
Density - Pressure Diagram Range of interestCopper3333



B) Copper 3333

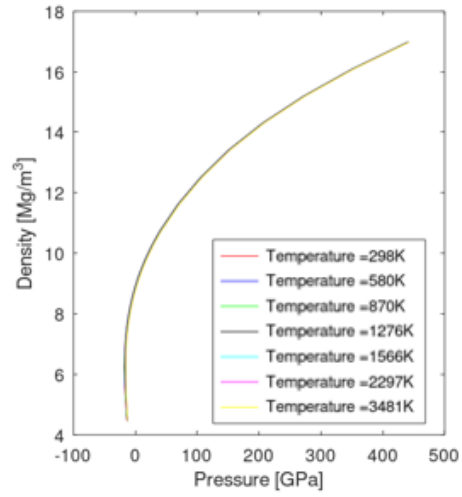


Density - Pressure Diagram Range of interestCopper3334



C) Copper 3334

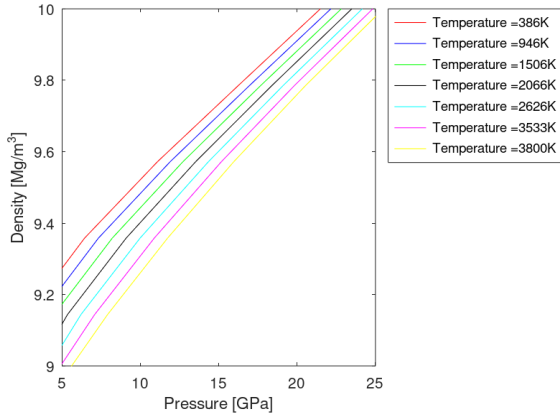
Density - Pressure Diagram Range of interestCopper3337



D) Copper 3337

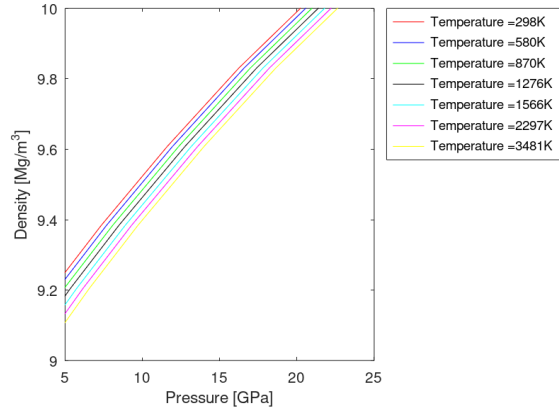
Figure 16 Density – Pressure diagrams in the range of interest for different copper tables

Density - Pressure Diagram Range of interestCopper3334



A) Copper 3334

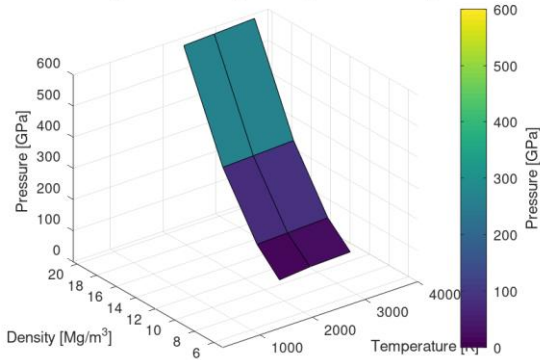
Density - Pressure Diagram Range of interestCopper3337



B) Copper 3337

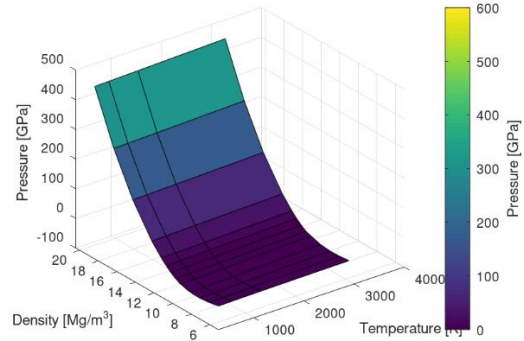
Figure 17 Zoomed Density – Pressure diagrams in the range of interest for different copper tables

erature - Density - Pressure Diagram Range of interestmolybdenum2983



A) Molybdenum 2983

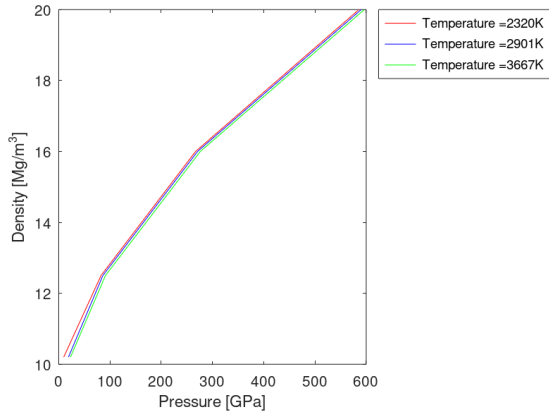
erature - Density - Pressure Diagram Range of interestmolybdenum2984



B) Molybdenum 2984

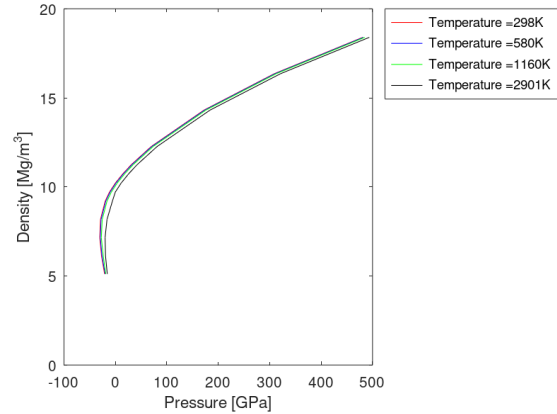
Figure 18 Temperature – Density – Pressure diagrams in the range of interest for different molybdenum tables

ensity - Pressure Diagram Range of interestmolybdenum2983



A) Molybdenum 2983

ensity - Pressure Diagram Range of interestmolybdenum2984



B) Molybdenum 2984

Figure 19 Density – Pressure diagrams in the range of interest for different molybdenum tables

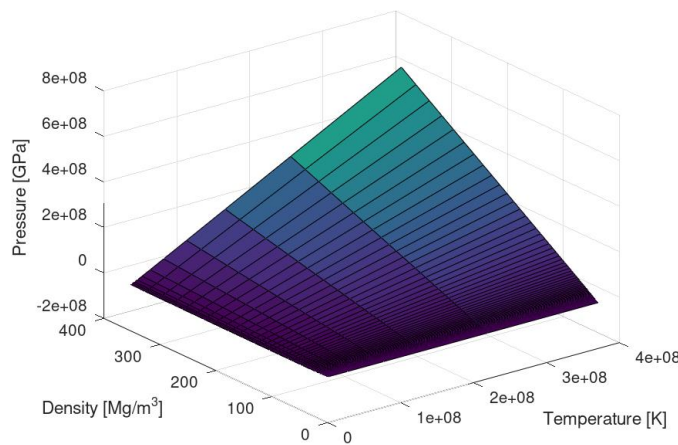
A comparison between the different tables for molybdenum was made (Figure 18 and Figure 19). Table 2984 has higher number of points in the range of interest than table 2983. It has more data in the area of low pressure and low density. Negative pressure is the result of a tensile force on the material.

Temperature – Density – Pressure Diagrams, Temperature – Density – Energy Diagrams and Density – Pressure diagrams for diamond 7830 (Figure 20 and Figure 21), carbon graphite 7833 (Figure 22 and Figure 23), and aluminum 3719 (Figure 24) are created.

Table diamond 7830 has limited number of points in the range of interest – only one temperature. Because of the relatively low influence of the temperature on the EOS, the table could be used in regions with higher temperatures.

Using the Old SESAME Library, carbon EOS (material number 2110) was investigated. Temperature – Density – Pressure Diagram is shown on Figure 25 and Density – Pressure diagram in the range of interest on Figure 26. The slope of the isotherms is negative. For higher temperatures the slope changes and the diagram get the expected shape.

Temperature - Density - Pressure DiagramDiamond7830



Temperature - Density - Energy DiagramDiamond7830

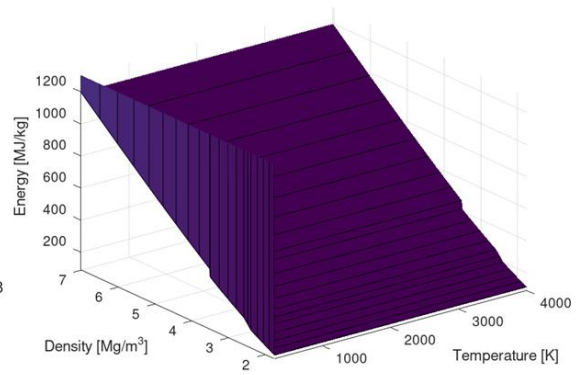


Figure 20 Temperature – Density – Pressure Diagrams and Temperature – Density – Energy Diagrams for diamond 7830

Density - Pressure Diagram Range of interestDiamond7830

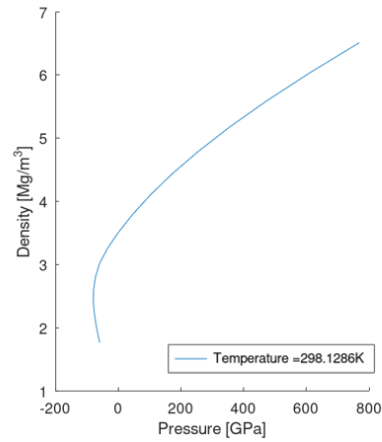
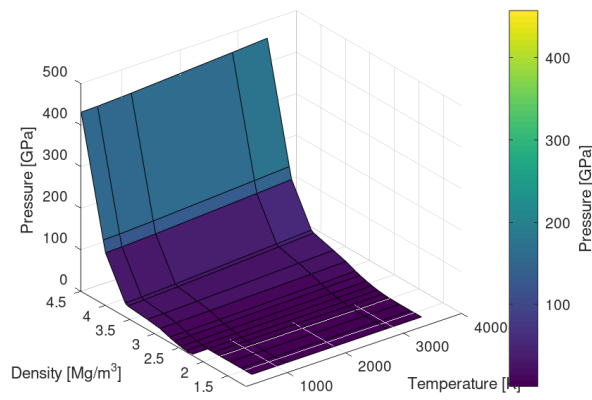


Figure 21 Density – Pressure diagrams for diamond 7830

Temperature - Density - Pressure Diagram Range of interestCarbon grafite7833



Temperature - Density - Energy Diagram Range of interestCarbon grafite7833

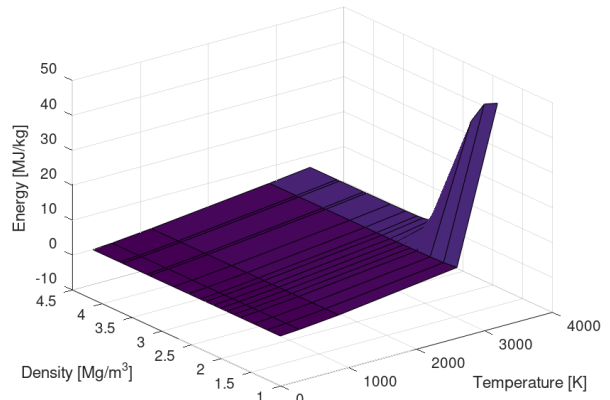


Figure 22 Temperature – Density – Pressure Diagrams and Temperature – Density – Energy Diagrams for carbon graphite 7833

Density - Pressure Diagram Range of interestCarbon grafite7833

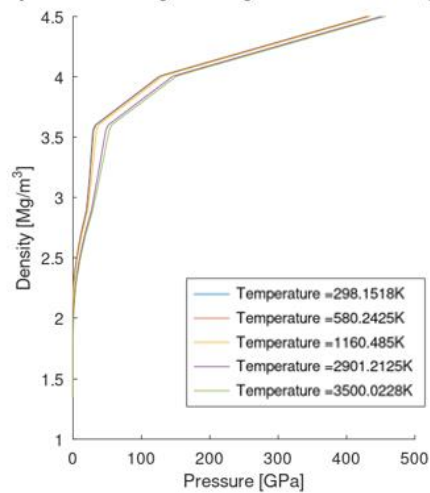
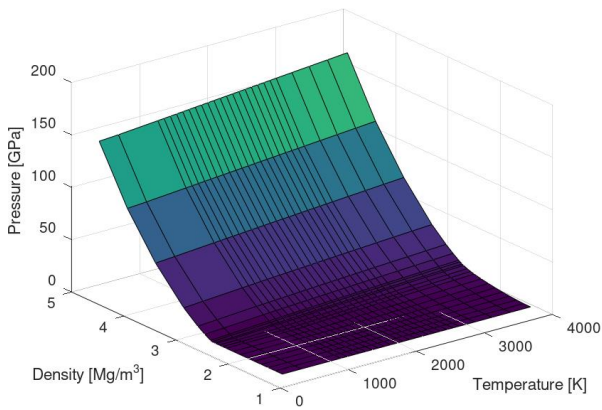


Figure 23 Density – Pressure diagrams for carbon graphite 7833

Temperature - Density - Pressure Diagram Range of interestAluminum3719



Temperature - Density - Energy Diagram Range of interestAluminum3719

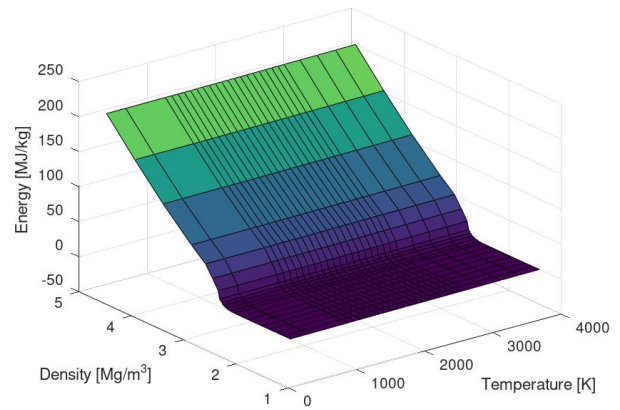


Figure 24 Temperature – Density – Pressure Diagrams and Temperature – Density – Energy Diagrams for aluminum 3719

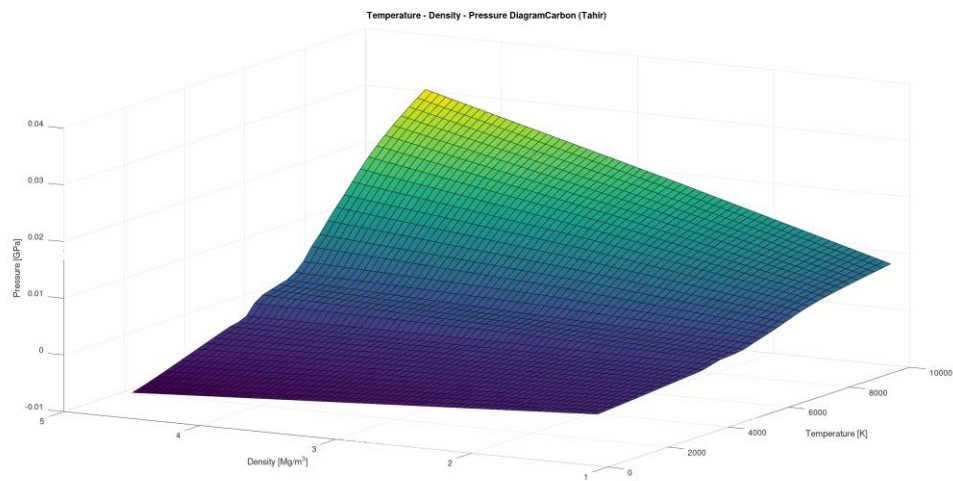


Figure 25 Temperature – Density – Pressure Diagram for carbon 2110

Density - Pressure Diagram Range of interestCarbon (Tahir)

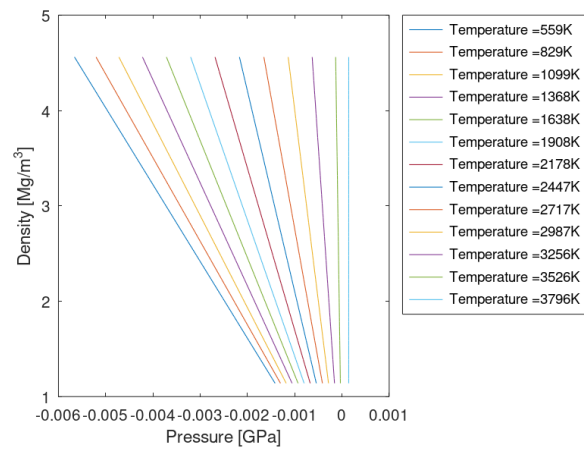


Figure 26 Density – Pressure Diagram in the range of interest for carbon 2110

## Matlab code for extracting data from the SESAME library – Equation of state comparison

The SESAME EOS for dry air table 5030 was compared with the ideal gas EOS (Figure 27). SESAME EOS and ideal gas EOS match in the region of high temperature and low pressure. For higher pressure the real gas EOS, or REFPROP software should be used.

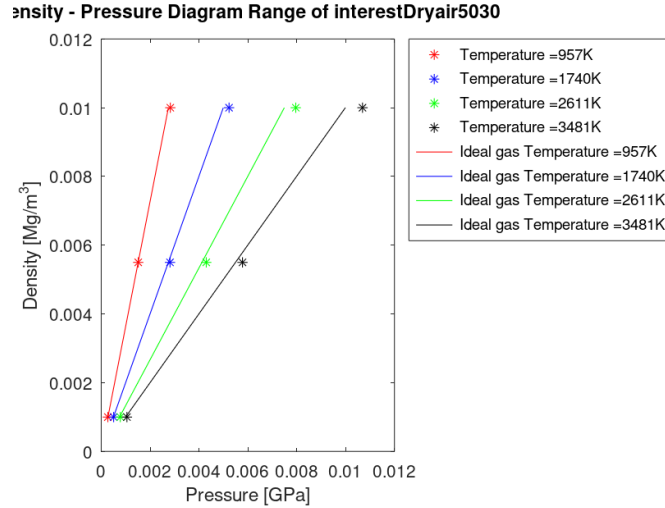


Figure 27 SESAME EOS Dry air table 5030 and ideal gas EOS comparison

The SESAME EOS for copper tables 3333 and 3337 were compared with the Mie-Gruneisen EOS and the Linear EOS (Figure 28). The parameters for the Mie-Gruneisen EOS and the Linear EOS are:  $\rho_0=8.93 \text{ g/cm}^3$ ;  $C_0=3.958 \text{ km/s}$ ;  $S=1.497$ ;  $K=137 \text{ GPa}$  [2]. In the area of pressure around 0 GPa and density below  $12 \text{ Mg/m}^3$  the Mie-Gruneisen EOS and the SESAME EOS 3337 match. In the area of around 0 GPa and densities 8 -  $10 \text{ Mg/m}^3$  the Linear EOS and the SESAME EOS 3337 match. In the SESAME EOS 3334 the isotherms are vertical in the area below the normal density and around 0 GPa pressure, and it does not match with the Mie-Gruneisen EOS.

Comparison between the carbon table EOS from the Old SESAME library with Mie-Gruneisen EOS and Linear EOS is made (Figure 29 A). The parameters for the Mie-Gruneisen and Linear EOS are  $\rho_0=1.85 \text{ g/cm}^3$ ,  $C_0=2.49 \text{ km/s}$ ;  $S=1.17$ ;  $K=3.33 \text{ GPa}$ . The Mie-Gruneisen EOS depends on the S value a lot.

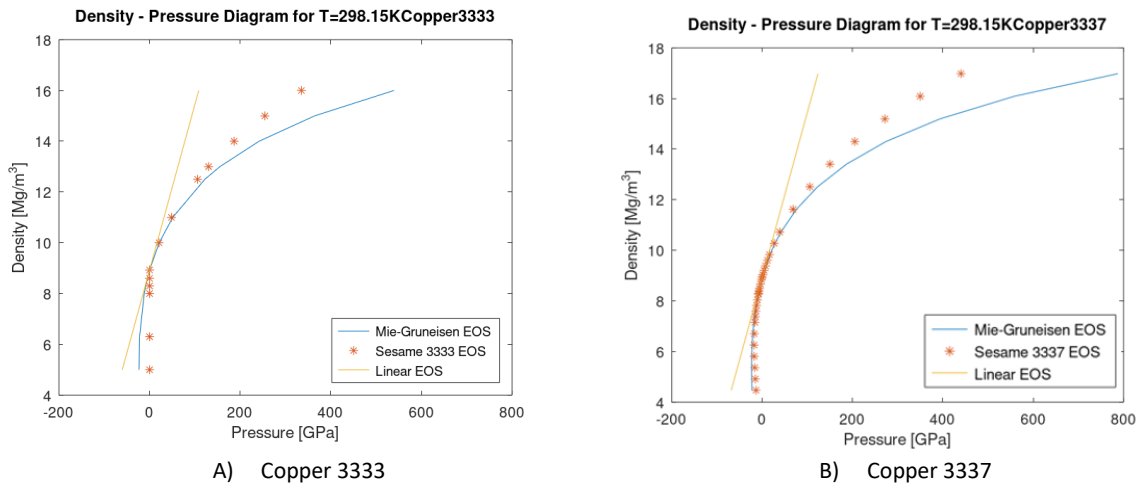


Figure 28 SESAME EOS Copper, Mie-Gruneisen EOS and Linear EOS comparison

The curves do not match for density higher than 2.5 g/cm<sup>3</sup>. A comparison with table graphite 7832 was carried out (Figure 29 B). The SESAME EOS table graphite 7832 matches with Mie-Grüneisen EOS with different S values in the tensile and compression region (Figure 30). The SESAME EOS table graphite 7832 matches with the Polito EOS and with the experimental data – blue dots (Figure 31).

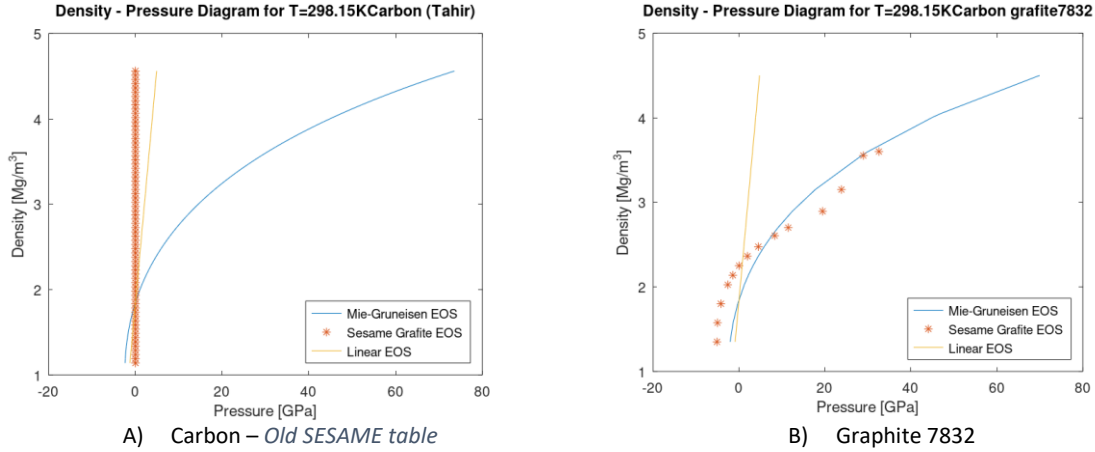


Figure 29 SESAME EOS Graphite, Mie-Grüneisen EOS and Linear EOS comparison

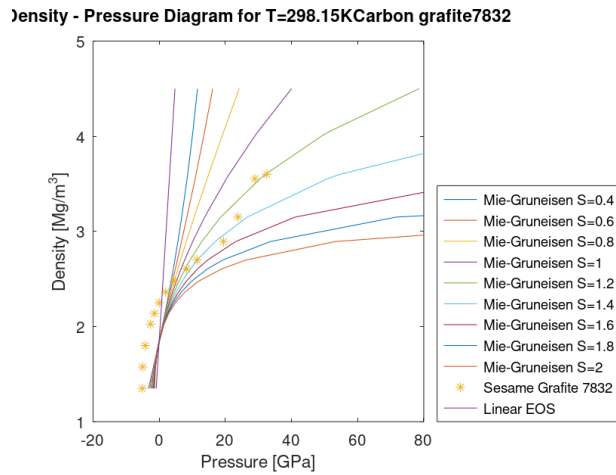


Figure 30 SESAME EOS Graphite, Mie-Grüneisen EOS with different S values and Linear EOS comparison

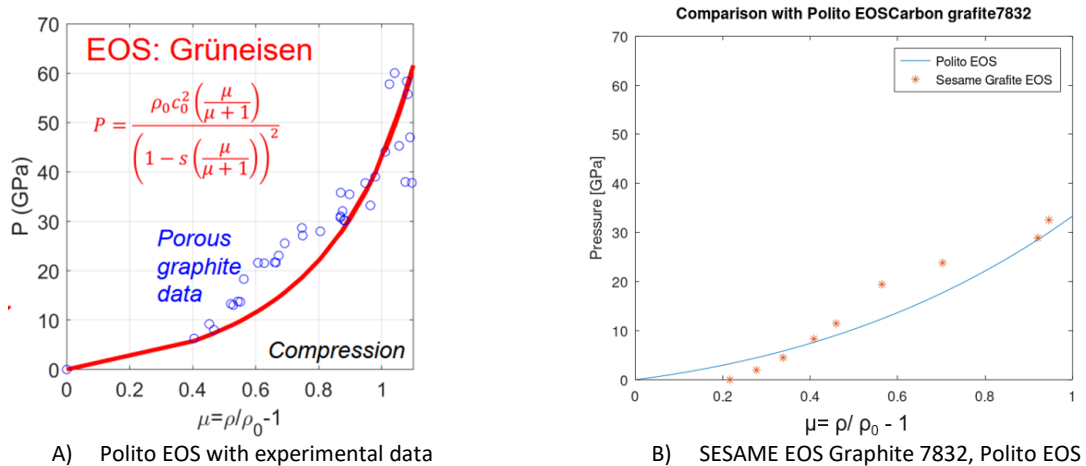


Figure 31 SESAME EOS Graphite, Polito EOS, experimental data comparison



## 7. AUTODYN simulations

Simulation of a hypervelocity, high-temperature impact on a material can be created using ANSYS and AUTODYN. AUTODYN enables simulation of short phenomena, high strain rate as well as shock wave more accurately. The model consists of: symmetry definition, material definition (EOS, strength, failure model, erosion and cutoffs), initial and boundary conditions definition, part definition, mesh definition (Lagrangian, Eulerian, Smooth Particle Hydrodynamics), gauges definition, cycle definition.

Simulations of a laser impact on a material are presented [6]. The part is axial symmetric. The mesh is Lagrangian. The boundary condition is defined as the stress on the front surface (pressure – time function), as well as zero velocity on the upper surface. The pressure – time function depends on the laser intensity (Figure 32) and the maximum pressure is chosen to be 100GPa. Strength and failure model are not added.

A simulation of a laser impact on 2mm graphite target is presented. The results show the change of temperature, pressure, density, internal energy, velocity in time, in given gauges (Figure 33; Figure 34).

Different EOS for the material can be chosen (SESAME EOS, Mie-Gruneisen EOS, Linear EOS) in AUTODYN. A simulation of a laser impact on 0.75mm copper target is carried out (Figure 35). The pressure wave and the relaxation wave are shown. The influence of the EOS on the simulation results is investigated.

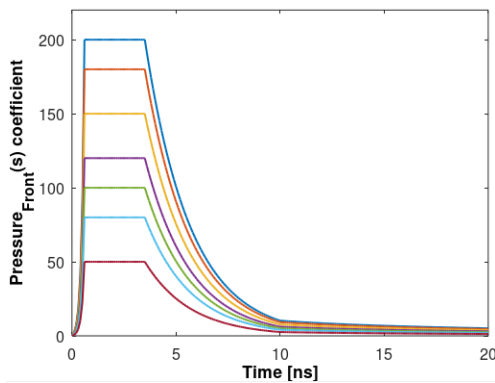


Figure 32 Pressure – time function for different laser intensity

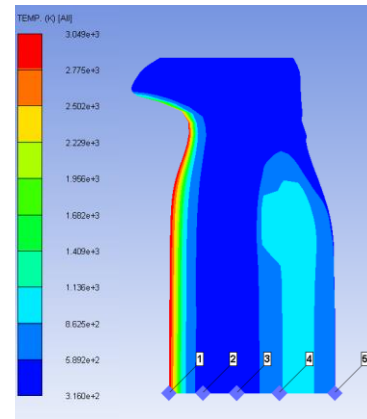
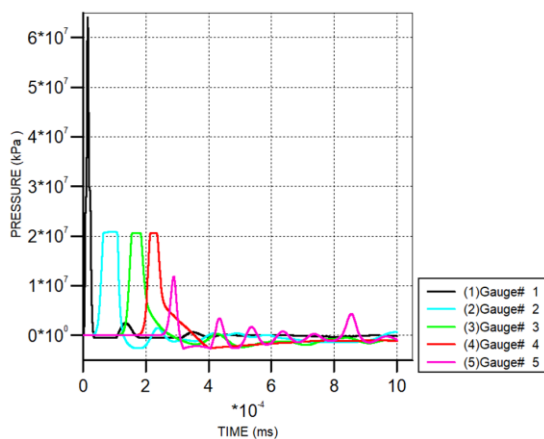


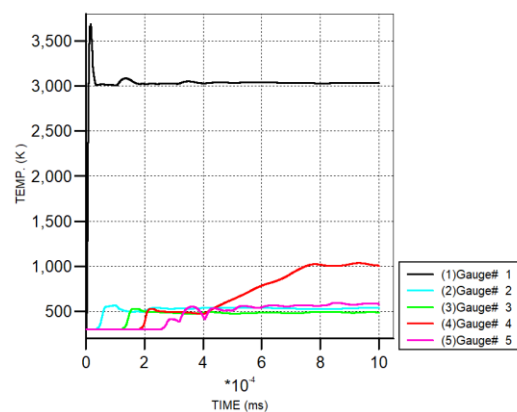
Figure 33 Temperature profile of graphite target

Gauge History ( Ident 0 - 2mm\_1d\_gsi )



A) Pressure - time

Gauge History ( Ident 0 - 2mm\_1d\_gsi )



B) Temperature-time

Figure 34 Results from the simulation on a carbon

The variations of pressure are similar when using different EOS (Figure 36). The values of the pressure are different, especially in the range of negative pressures. The SESAME EOS table copper 3333 is not defined in the negative pressure area and cannot be used for simulation of a tensile forces. The SESAME EOS table copper 3337 should be added in AUTODYN.

The variations of velocity are similar for Linear and Mie-Gruneisen EOS, but different from the SESAME EOS (Figure 37). Different values of velocity are obtained when using SESAME EOS, compared to Linear and Mie-Gruneisen EOS.

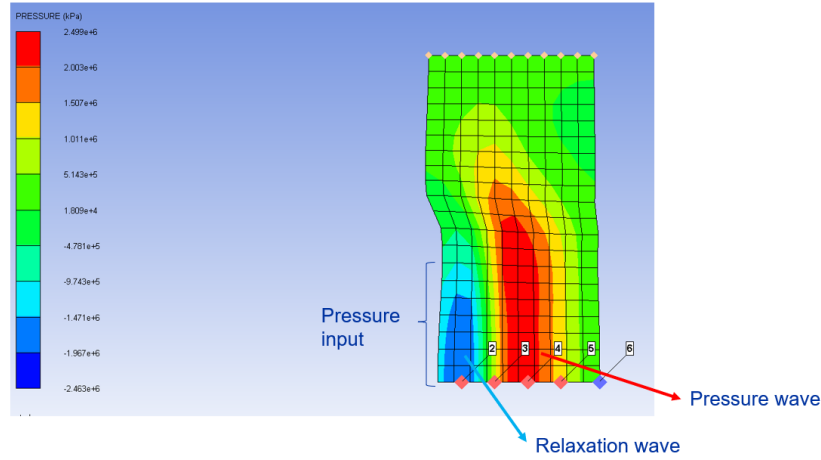


Figure 35 Pressure change in copper under laser impact

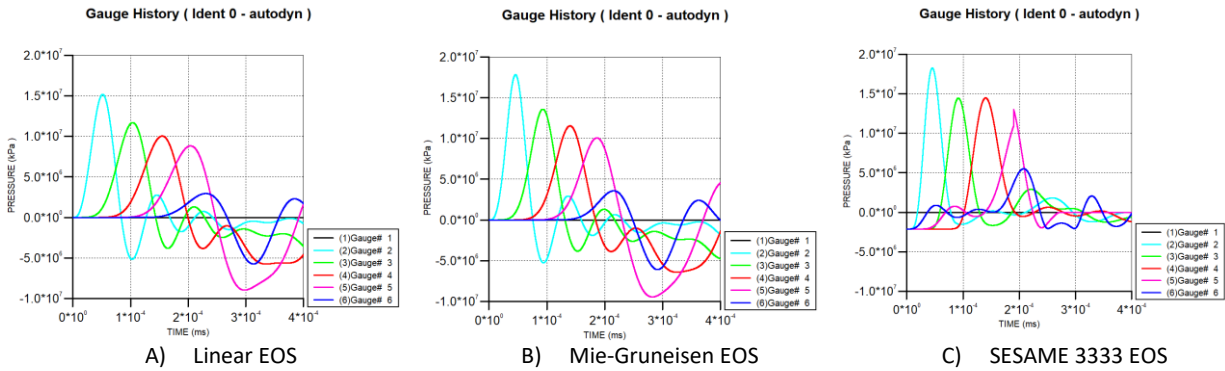


Figure 36 Influence of the EOS on the simulation results: pressure - time

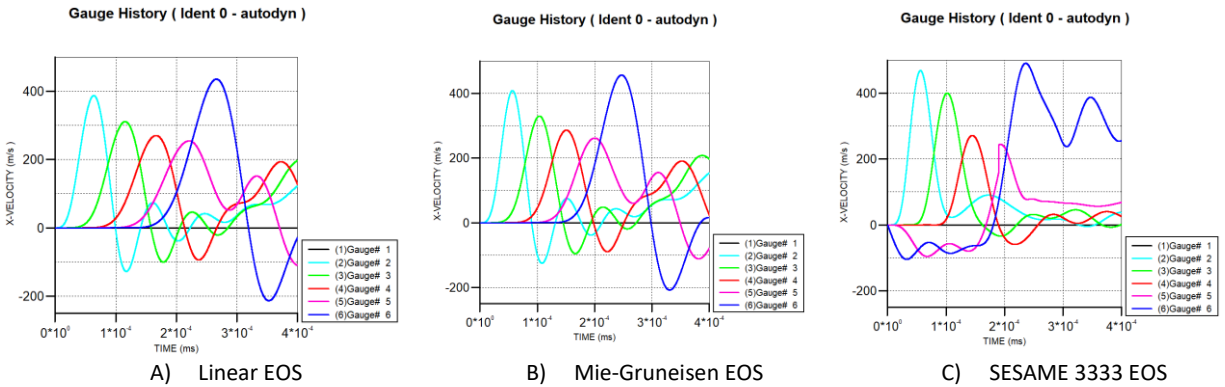


Figure 37 Influence of the EOS on the simulation results: x-velocity - time



## 8. Conclusions

The recent progress in the equation of state and constitutive models for various materials is presented.

High energy particle beams impact into the target material causing thermodynamic states of high compression and expansion and strong thermomechanical phenomena: high pressures and temperatures, elastic, plastic and shock wave behavior, changes of material density, phase (solid-liquid-gas-plasma) transitions, intense stress waves, material fragmentation and explosions.

A Matlab code is developed in this work, and equation of state diagrams are presented using SESAME EOS files. A comparison between the Old SESAME Library and the New SESAME Library was made. The equations of state for existing materials in the New SESAME Library are upgraded, and equations of state for new materials are added. The new tables contain higher number of points in the range of interest which leads to more accurate EOS. Particularly valuable is the new table for copper 3337, because of its application as material for the beam dump. Negative pressure, as the result of a tensile force on the material, appears in the new table for copper 3337, diamond 7830, molybdenum, and some other materials. For many materials, in the area below the normal density and around 0 GPa pressure, the isotherms are vertical.

The influence of the temperature on the EOS is relatively low. The table diamond 7830 has limited number of points in the range of interest – only one temperature. Because of the relatively low influence of the temperature on the EOS, the table could be used in regions with higher temperatures.

A comparison to linear equation of state and Mie-Grüneisen equation of state is realized. Acceptable coincidence with SESAME EOS is obtained in regions of low pressures and in regions without phase transitions. The data from table copper 3337 match with Mie-Grüneisen EOS in the area of low pressure and low density.

Simulations of laser beam impact on different materials using different EOS are carried out. The Sesame library can be used for simulation of a hypervelocity high-temperature impact on a target in Ansys AUTODYN. For simulation in AUTODYN the new table for copper 3337, or Mie-Grüneisen EOS could be used. Table 3337 has not been integrated in AUTODYN yet. The simulation results show that the variations of pressure are similar when using different EOS, but the values of the pressure are different, especially in the range of negative pressures. The SESAME EOS table copper 3333 is not defined in the negative pressure area and cannot be used for simulation of a tensile forces. The SESAME EOS table copper 3337 should be added in AUTODYN. The variations of velocity are similar for Linear and Mie-Grüneisen EOS, but different from the SESAME EOS. Different values of velocity are obtained when using SESAME EOS, compared to Linear and Mie-Grüneisen EOS.

## Acknowledgement

I would like to thank my supervisors, Federico Carra, PhD and Lucie Baudin, PhD for their guidance during the summer student program and Prof. Michele Pasquali, PhD for the helpful suggestions. I would like to thank CERN for organizing this summer student program, CERN & Society Foundation for funding my participation and my home university Ss Cyril and Methodius University, Faculty of Mechanical Engineering, Skopje, R. Macedonia.

## References

- [1] J. R. Asay, G. I. Kerley, The response of materials to dynamic loading, *Int. J. Impact Engng*, 1987
- [2] F. Carra, Thermomechanical Response of Advanced Materials under Quasi-Instantaneous Heating, PhD Thesis, Politecnico di Torino, 2017
- [3] F. Carra et al., Behaviour of advanced materials impacted by high energy particle beams, *Journal of Physics: Conference Series*, 2013
- [4] F. Carra et al., The “Multimat” experiment at CERN HiRadMat facility: advanced testing of novel materials and instrumentation for HL-LHC collimators, *Journal of Physics: Conference Series*, 2017
- [5] L. Baudin, PHELIX – Autodyn Simulations, CERN, Engineering department
- [6] L. Baudin, A simulation model for material response under laser beam impact, CERN, Engineering department
- [7] C. T. Martin et al., First observation of spalling in tantalum at high temperatures induced by high energy proton beam impacts, *European Journal of Mechanics / A Solids*, 2021
- [8] SESAME: The Los Alamos National Laboratory Equation of state Database, 1995
- [9] M.J. Moran, H.N. Shapiro, D.D. Boettner, M.B. Bailey, Fundamentals of Engineering Thermodynamics, John Wiley & Sons, 2014
- [10] A. Bertarelli, Beam-induced damage mechanisms and their calculation, CERN Yellow Reports, 2016